Supporting Information

Fabrication and Photocatalytic Applications of Perovskite Materials with Special Emphasis on Alkali Metal based Niobates and Tantalates

Tokeer Ahmad*, Umar Farooq and Ruby Phul

Nanochemistry laboratory, Department of Chemistry, Jamia Millia Islamia, New Delhi-110025, INDIA

*To whom correspondence should be addressed: Email: tahmad3@jmi.ac.in (T. Ahmad)
Phone: 91-11-26981717, Extn: 3261

Table S1: Reaction conditions used during synthesis of alkali niobates and tantalates by solid state reactions.

Material	Solvent	Precursor	Conditions	Product description	Ref.
$0.98K_{0.48}Na_{0.52}Nb_{0.96}Sb_{0.04}$-0.02 $Bi_{0.5}Na_{0.5}HfO_3$	Alcohol	K_2CO_3, Na_2CO_3 Nb_2O_5, Sb_2O_3, Bi_2O_3, $CaCO_3$, ZrO_2, HfO_2 and TiO_2	850 °C for 6 h,1080 & 1075 °C 3h	NA	S1
(0.995-x) KNN-0.005BS-xBNKLZ (x= 0-0.07)	Alcohol	Na_2CO_3, K_2CO_3, Bi_2O_3,Nb_2O_5, Li_2CO_3, Sc_2O_3 and ZrO_2	1080-1150°C 3 h in air	NA	S2
$0.992(K_{0.46}Na_{0.54})_{0.965}Li_{0.035}Nb1-xSb_xO_3$-$_{0.008}BiScO_3$	Ethanol	Na_2CO_3, K_2CO_3, Li_2CO_3, Nb_2O_5, Bi_2O_3, Sc_2O_3, and Sb_2O_3.	850 °C, 6 h	Depends on amount of x	S3
$Na_{0.47}K_{0.47}Li_{0.06}NbO_3$	NA	K_2CO_3, Na_2CO_3, Nb_2O_5 and Li_2CO_3.	850 °C, 10 h	700 nm to 4 μm	S4
$NaTaO_3$ and the doped $NaTaO_3$: La	NA	Ta_2O_5, Na_2CO_3, La_2O_3	1170 K, 1 h and 1420 K, 10 h	2−3 μm and 0.1−0.7 μm	S5
Fe-Doped $NaTaO_3$	NA	Ta_2O_5, Na_2CO_3, Fe_2O_3	900 °C, 1 h and 1150 °C, 10 h	NA	S6
$ATaO_3$ (A) Li, Na, and K)	NA	Li_2CO_3, Na_2CO_3, K_2CO_3, Ta_2O_5,	1420 K, 10 h	Effected by concentration of alkali	S7
$NaTaO_3$ and metal-doped $NaTaO_3$ ($NaTaO_3$:M)	Acetone	Na_2CO_3, Ta_2O_5, La_2O_3, Nd_2O_3, Y_2O_3, Yb_2O_3, $CaCO_3$, $SrCO_3$, $BaCO_3$	120 rpm for 24 h, drying at (333 K), calcined in air at 1173 K, 1 h and 1373 K, 10 h	400-600 μm.	S8

Material	Solvent	Precursor	Conditions	Product description	Ref.
$NaTaO_3$	NA	Na_2CO_3, Ta2O_5, La_2O_3, $Ni(NO_3)_2$	calcined at 1420 K in air, NiO impregnation at 540 K,573 K in 20-Torr O2	2 µm	S9
Strontium-doped $NaTaO_3$	NA	Na_2CO_3, Ta_2O_5, $SrCO_3$,	1173 K, 1 h and then at 1423 K, 10 h	Varies with etching time	S10
Eu^{3+}-doped $NaTaO_3$	HCl, H2O	TaCl, $Eu(NO_3)_3$, NaCO3	900 °C, 9 h.	~65 nm for NaNbO3	S11
Lanthanum-Doped $NaTaO_3$ Photocatalyst	NA	La_2O_3, Na_2CO_3, Ta_2O_5	1170 K, 1 h and 1420 K for 10 h with intermediate grinding	0.1-0.7 µm	S12
Fe doped $NaTaO_3$ and $LaFeO_3$−$NaTaO_3$	acetone	Ta_2O_5, Na_2CO_3, Fe_2O_3, La_2O_3	1173 and 1473 K, 10 h	20−50 nm	S13
$NaTaO_3$, Bi–$NaTaO_3$ and Bi_2O_3/Bi–$NaTaO_3$	NA	$Na_2C_2O_4$, Ta_2O_5, $Bi(NO_3)_3.5H_2O$, urea	600 °C, 4 h	greater than 100 nm	S14
Ni,Co-Doped $LiNbO_3$ and LiTaO3	acetone	Li_2CO_3, Nb_2O_5, Ta_2O_5, CoO, and NiO.	700 °C, 2 h, to expel CO2, at 800 and 900 °C for 1 h each, and finally heated at 1000-1250 °C,	NA	S15
$NaNb_xTa_{1-x}O_3$ (x = 0, 0.25, 0.5, 0.75, 1	NA	Na_2CO_3, Ta_2O_5 and Nb_2O_5	900 °C, 12 h	100–500 nm	S16
$InFeO_3$	NA	Fe_2O_3, In_2O_3,	15 GPa and 1450 °C	25 µm	S17

Material	Solvent	Precursor	Conditions	Product description	Ref.
$ZnSnO_3$	NA	ZnO and SnO_2	7 GPa and 1000 °C, 30 min		S18
$K_{0.5}Na_{0.5}NbO_3$	ethanol	K_2CO_3, Na_2CO_3, Nb_2O_5	220°C, 5 h, 800 °C (in air), 2 h	1.2 μm	S19
Mn-doped $K_{0.5}Na_{0.5}NbO_3$ ceramics	ethanol	K_2CO_3, Na_2CO_3, Nb_2O_5, MnO	220 °C, 5 h, 800 °C (in air), 2 h	1.8 μm	S20
$(K_{0.44}Na_{0.52}Li_{0.04})$ $[(Nb_{0.86}Ta_{0.10}Sb_{0.04})1$ $xW_{5x/6}]$ O_3	ethanol	Na_2CO_3, Li_2CO_3, K_2CO_3, WO_3, Nb_2O_5, Ta_2O_5, and Sb_2O_5	700 °C, 2 h at 3 °C min^{-1}	4 μm	S21
(1-x) $(K_{0.5}Na_{0.5})$ NbO_3– $xBi(Mg_{2/3}Nb_{1/3})$ O_{33} (x ¼ 0, 0.05, 0.10, 0.15 and 0.20 mol)	alcohol	K_2CO_3, Na_2CO_3, Bi_2O_3, Nb_2O_5, and MgO	950 °C, 5 h., 1120-1220 °C, 5 h	1 μm	S22
(1−x) $(K_{0.48}Na_{0.52})$ $(Nb_{0.96}Sb_{0.04})O_3$-x $[Bi_{0.5}(Na_{0.7}Ag_{0.3})_{0.5}]$ 0.90-$Zn_{0.10}ZrO_3$ (x = 0, 0.01, 0.02, 0.03, 0.035, 0.04, 0.0425, 0.045, 0.05, and 0.06)	anhydrous ethanol	K_2CO_3, Na_2CO_3, Nb_2O_5, Bi_2O_3, ZnO, Ag_2O, Sb_2O_3, and ZrO_2	850 °C, 6 h, 1040–1120 °C, 2 h	Depends on x	S23
$KNbO_3$	NA	K_2CO_3, Nb_2O_5	650–925°C, 10 h. 1150 °C, 10 h.	28, 32 and 39 nm at 650,725, and 900C respectively	S24

Table S2: Reactions conditions during hydrothermal synthesis and particle size of lead free pervoskites/ piezoelectric materials.

Material	Solvent	Precursor	Reaction conditions	Particle size	Ref
Niobate Nanowire	H_2O	Nb_2O_5, NaOH	120 °C, 3 h	100 nm & length of several hundred microns	S25
$NaNbO_3$ N-doped $NaNbO_3$	H_2O PTFE	Nb_2O_5 (2g) NaOH urea	200°C, 250 min 600 °C, 0.5 h	700nm/ depends on amount of urea	S26
$NaNbO_3$	H_2O PTFE	Nb_2O_5 (2 g) NaOH	200 °C, 250 min	700nm	S27
$(Na_xK_{1-x})NbO_3$ (NKN)	H_2O	Nb_2O_5, NaOH, KOH	200 °C, 24 h	NA	S28
$KNbO_3$	H_2O	Nb_2O_5 KOH	150-200 °C	100-300 nm & length up to 5 mm	S29
Ag_2O grafted sodium niobate nanofibers	H_2O	$Nb_2Na_2O_6 \cdot H_2O$ Nb_2O_5, NaOH, silver nitrate	180 °C, 2 h	3-5 nm	S30
sodium niobate nanoparticles	H_2O/ethylene glycol	Nb_2O_5, KOH, NaOH	220 °C, 4 h	NA	S31
$XNbO_3$ ($NaNbO_3$, $KNbO_3$, &$LiNbO_3$)	H_2O	Nb_2O_5 (KOH, NaOH, LiOH)	150 to 200°C 0.5 to 72 h.	NA	S32
sodium niobate		(Nb_2O_5), (KOH), (NaOH),	120, 160, 180, 200, 220 & 240°C	50-100mm	S33
$KNbO_3$		Nb_2O_5, KOH	200°C, 12 h	100–600 nm	S34
$NaNbO_3$ g-C_3N_4/$NaNbO_3$	H_2O	P123 ($EO_{20}PO_{70}EO_{20}$), $Nb(OC_2H_5)_5$, NaOH	40 °C, 2 h, 200 °C, 24 h, 550 °C, 4 h 520 °C, 4h	~200 nm & length up to several tens μm	S35
$KNbO_3$ Nanowires	H_2O	Nb powder, KOH	150 °C, 12 h	Thickness 74.0 ± 11.7 nm & length 5.1 ± 1.4 μm	S36
$ATaO_3$ and $ANbO_3$ (A=Na and K)	H_2O	Ta_2O_5, Nb_2O_5, NaOH and KOH	240 °C, 24 h	200 nm.	S37

Table S3: UV-Light-Active Photocatalysts for Water Splitting to Hydrogen and/or Oxygen.

Photocatalyst	B.G	Rate ($mmolh^{-1}g^{-1}$)	Sacrificial Reagent	Rate ($mmol\ h^{-1}g^{-1}$)	Sacrificial reagent	Cocatalyst	Quantum Yields	Ref
Cubic $NaNbO_3$	3.29	-	-	423	Methanol	-	-	S12
Cubic $NaNbO_3$	3.29	-	-	425	-	0.5wt% Pt	-	
Orthorhombic $NaNbO_3$	3.45	-	-	241	-	-	-	
Cubic $NaNbO_3$	3.29	-	-	520	-	1wt% Pt	-	
Cubic $NaNbO_3$	3.29	-	-	324	-	1.5wt% Pt	-	
$NaTaO_3$	4.0	0.78	$AgNO_3$	10.3	Methanol	-	-	S37
2 mol% La doped $NaTaO_3$	4.09	1.7	-	13.2	-	-	56% at 270 nm	

Photocatalyst	B.G	Rate ($mmolh^{-1}g^{-1}$)	Sacrificial Reagent	Rate ($mmol\ h^{-1}g^{-1}$)	Sacrificial reagent	Cocatalyst	Quantum Yields	Ref
$NaNbO_3$	3.08	-	-	950	Methanol	-	-	S37
$KNbO_3$	3.14	-	-	100	-	-	-	
$NaTaO_3$	3.96	-	-	36750	-	-	-	
$KTaO_3$	3.42	-	-	1040	-	-	-	
$CaTiO_3$	-	-	-	670.1	Methanol NiO_x	-	-	S38
$NaTaO_3$	4.1	900	-	2050	-	-	-	S39
$NaTaO_3$	4.0	6	-	13	-	-	-	

Photocatalyst	B.G	Rate ($mmolh^{-1}g^{-1}$)	Sacrificial Reagent	Rate ($mmol\ h^{-1}g^{-1}$)	Sacrificial reagent	Cocatalyst	Quantum Yields	Ref
2 mol% Ca doped $NaTaO_3$	4.11	113	$AgNO_3$	756	Methanol	-	-	S40
2 mol% Sr doped $NaTaO_3$	4.11	186	-	830	-	-	-	
2 mol% Ba doped $NaTaO_3$	4.09	160	-	696	-	-	-	
$NaTaO_3$	4.03	40	-	563	-	-	-	S41
$NaTaO_3$	4.0	1000	-	-	-	-	-	
$NaTaO_3$	4.0	400	-	-	-	-	-	

Photocatalyst	B.G	Rate ($mmolh^{-1}g^{-1}$)	Sacrificial Reagent	Rate ($mmol\ h^{-1}g^{-1}$)	Sacrificial reagent	Cocatalyst	Quantum Yields	Ref
$Sr_{0.5}TaO_3$	3.7	177	-	733	-	-	-	S42
Re-$Sr_{0.5}TaO_3$	3.7	366	-	1400	-	-	-	
$NaNb_{0.5}Ta_{0.5}O_3$	3.6	37.8	-	-	-	0.125wt% of Pt	-	S16

Table S4. Amount of Ammonium Hydroxide Solution, Surface Areas, Band Gap Energies, and Hydrogen Production Rates after 2 h from Water Splitting Using Methanol as Sacrificial Agent sample NH_4OH.

Sample	NH_4OH solution (mL)	SBET ($m^2\ g^{-1}$)	band gap energy (eV)	H_2 rate (mmol h^{-1})	APA[a] (μmol g^{-1} L^{-1} h^{-1} W^{-1})
0-NaTa	0.00	200	4.4(amorphous)	2.4	800
0.25-NaTa	0.25	236	4.6 (amorphous) + 4.1 ($NaTaO_3$)	3.6	1200
1.6-NaTa	1.60	83	4.6 (amorphous) + 4.1 ($NaTaO_3$)	3.0	1000
3.2-NaTa	3.20	54	4.6 (amorphous) + 4.1 ($NaTaO_3$)	1.5	500
4.0-NaTa	4.00	26	4.1 ($NaTaO_3$) + 4.8 ($Na_2Ta_2O_6$)	1.4	470
4.8-NaTa	4.80	26	4.0 ($NaTaO_3$) + 4.9 ($Na_2Ta_2O_6$)	1.1	370
9.6-NaTa	9.60	29	4.8 ($Na_2Ta_2O_6$)	1.0	330
SS-$NaTaO_3$	–	2	4.0 ($NaTaO_3$)	0.8	270

[a]= Apparent photocatalytic activity (APA) calculated according to eq 1.

$$\mathrm{APA} = \frac{\text{moles of H2 evolution(mol)}}{\mathrm{XYZW}} \qquad (1)$$

Where X = weight of catalyst (g), Y = volume of reactant (L), Z = duration of reaction (h), and W = power of lamp (W).

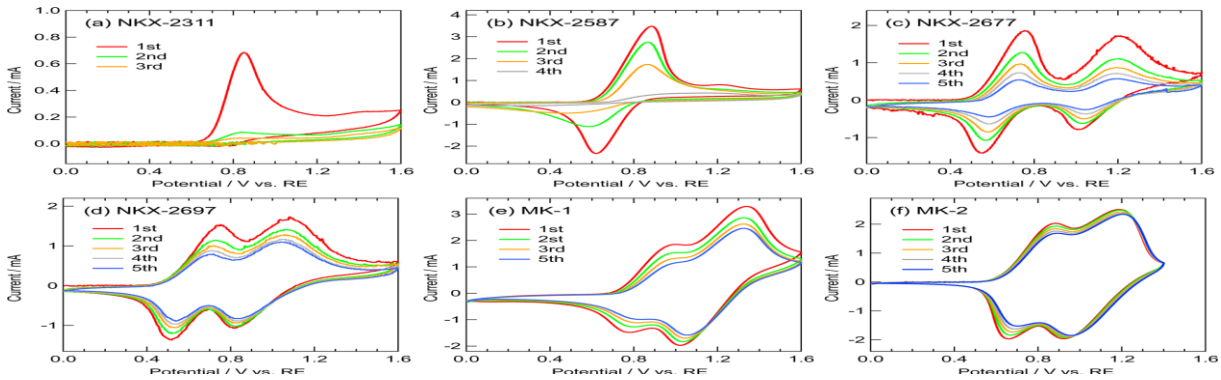

Figure S1 Wide range CV profiles of dyes adsorbed on a porous TiO_2 electrode in dehydrated acetonitrile containing 0.1 M $LiClO_4$ as a supporting electrolyte. The scan rate was 100 mVs^{-1}. Ag/Ag^+ in 0.01 M $AgNO_3$ acetonitrile solution was used as a reference electrode. [Reprinted with permission from ref. S43 Abe, R.; Shinmei, K.; Koumura, N.; Hara, K.; Ohtani, B., J. Am. Chem. Soc., 2013, 135, 16872. Copyright (2013) American Chemical Society.]

References:

(S1) Zheng, T.; Wu, J. Relationship between Poling Characteristics and Phase Boundaries of Potassium-Sodium Niobate Ceramics. ACS Appl. Mater. Interfaces 2016, 8, 9242.

(S2) Cheng, X.; Wu, J.; Lou, X.; Wang, X.; Wang, X.; Xiao, D.; Zhu, J. Achieving Both Giant d33 and High TC in Potassium-Sodium Niobate Ternary System. ACS Appl. Mater. Interfaces 2014, 6, 750.

(S3) Cheng, X.; Wu, J.; Wang, X.; Zhang, B.; Lou, X.; Wang, X.; Xiao, D.; Zhu, J. Mediating the Contradiction of d33 and TC in Potassium-Sodium Niobate Lead-Free Piezoceramics. ACS Appl. Mater. Interfaces 2013, 5, 10409.

(S4) Gupta, M. K.; Kim, S.-W.; Kumar, B. Flexible High-Performance Lead-Free $Na_{0.47}K_{0.47}Li_{0.06}NbO_3$ Microcube-Structure-Based Piezoelectric Energy Harvester. ACS Appl. Mater. Interfaces 2016, 8, 1766.

(S5) Phivilay, S. P.; Puretzky, A. A.; Domen, K.; Wachs, I. E. Nature of Catalytic Active Sites Present on the Surface of Advanced Bulk Tantalum Mixed Oxide Photocatalysts. ACS Catal. 2013, 3, 2920.

(S6) Zhou, X.; Shi, J.; Li, C. Effect of Metal Doping on Electronic Structure and Visible Light Absorption of $SrTiO_3$ and $NaTaO_3$ (Metal = Mn, Fe, and Co). J. Phys. Chem. C 2011, 115, 8305.

(S7) Sayama, K.; Arakawa, H. Photocatalytic Decomposition of Water and Photocatalytic Reduction of Carbon Dioxide over Zirconia Catalyst. J. Phys. Chem. 1993, 97, 531.

(S8) H. Photocatalytic Steam Reforming of Methane over Sodium Tantalate. J. Phys. Chem. C 2010, 114, 3493.

(S9) Yamakata, A.; Ishibashi, T.-a.; Takeshita, K.; Onishi, H. Time-resolved Infrared Absorption Study of Photochemical Reactions Over Metal Oxides. Top. Catal. 2005, 35, 211.

(S10) An, L.; Park, Y.; Sohn, Y.; Onishi, H. Effect of Etching on Electron−Hole Recombination in Sr-Doped $NaTaO_3$ Photocatalysts. J. Phys. Chem. C 2015, 119, 28440.

(S11) Su, Y.; Peng, L.; Guo, J.; Huang, S.; Lv, L.; Wang, X. Tunable Optical and Photocatalytic Performance Promoted by Nonstoichio-metric Control and Site-Selective Codoping of Trivalent Ions in NaTaO3. J. Phys. Chem. C 2014, 118, 10728.

(S12) Kato, H.; Asakura, K.; Kudo, A. Highly Efficient Water Splitting into H_2 and O_2 over Lanthanum-Doped $NaTaO_3$ Photocatalysts with High Crystallinity and Surface Nanostructure. J. Am. Chem. Soc. 2003, 125, 3082.

(S13) Kanhere, P.; Nisar, J.; Tang, Y.; Pathak, B.; Ahuja, R.; Zheng, J.; Chen, Z. Electronic Structure, Optical Properties, and Photocatalytic Activities of $LaFeO_3$-$NaTaO_3$ Solid Solution. J. Phys. Chem. C 2012, 116, 22767.

(S14) Reddy, K. H.; Martha, S.; Parida, K. M. Facile Fabrication of Bi_2O_3/Bi-$NaTaO_3$ Photocatalysts for Hydrogen Generation Under Visible Light Irradiation. RSC Adv. 2012, 2, 9423.

(S15) Paul, M.; Tabuchi, M.; West, A. R. Defect Structure of Ni,Co-Doped $LiNbO_3$ and $LiTaO_3$. Chem. Mater. 1997, 9, 3206.

(S16) Jana, P.; de la Pena O'Shea, V. A.; Montero, C. M.; Galὺez, P.; Pizarro, P.; Coronado, J. M.; Serrano, D. P. Mixed $NaNb_xTa_{1-x}O_3$ Perovskites as Photocatalysts for H_2 Production. Green Chem. 2015, 17, 1735.

(S17) Fujita, K.; Kawamoto, T.; Yamada, I.; Hernandez, O.; Hayashi, N.; Akamatsu, H.; Lafargue-Dit-Hauret, W.; Rocquefelte, X.; Fukuzumi, M.; Manuel, P.; Studer, A. J.; Knee, C. S.; Tanaka, K. $LiNbO_3$-Type $InFeO_3$: Room-Temperature Polar Magnet without Second-Order Jahn-Teller Active Ions. Chem. Mater. 2016, 28, 6644.

(S18) Inaguma, Y.; Yoshida, M.; Katsumata, T. A Polar Oxide $ZnSnO_3$ with a $LiNbO_3$-Type Structure. J. Am. Chem. Soc. 2008, 130,2000 6704.

(S19) Mahajan, A.; Pinho, R.; Dolhen, M.; Costa, M. E.; Vilarinho, P. M. Unleashing the Full Sustainable Potential of Thick Films of Lead-Free Potassium Sodium Niobate ($K_{0.5}Na_{0.5}NbO_3$) by Aqueous Electrophoretic Deposition. Langmuir 2016, 32, 5241.

(S20) Rafiq, M. A.; Tkach, A.; Costa, M. E.; Vilarinho, P. M. Defects and Charge Transport in Mn-doped $K_{0.5}Na_{0.5}NbO_3$ ceramics. Phys. Chem. Chem. Phys. 2015, 17, 24403.

(S21) Ramajo, L.; Castro, M.; del Campo, A.; Fernandez, J. F.; Rubio-Marcos, F. Revealing the Role of Cationic Displacement in Potassium-Sodium Niobate Lead-Free Piezoceramics By Adding W^{6+} Ions. J. Mater. Chem. C 2015, 3, 4168−4178.

(S22) Shao, T.; Du, H.; Ma, H.; Qu, S.; Wang, J.; Wang, J.; Wei, X.; Xu, Z. Potassium−Sodium Niobate Based Lead-Free Ceramics: Novel Electrical Energy Storage Materials. J. Mater. Chem. A 2017, 5, 554−563.

(S23) Wang, Y.; Hu, L.; Zhang, Q.; Yang, H. Phase Transition Characteristics and Associated Piezoelectricity of Potassium-Sodium Niobate Lead-Free Ceramics. Dalton Trans. 2015, 44, 13688.

(S24) Choi, J.; Ryu, S. Y.; Balcerski, W.; Lee, T. K.; Hoffmann, M. R. Photocatalytic Production of Hydrogen on Ni/NiO/$KNbO_3$/CdS Nanocomposites Using Visible Light. J. Mater. Chem. 2008, 18, 2371.

(S25) Ke, T.-Y.; Chen, H.-A.; Sheu, H.-S.; Yeh, J.-W.; Lin, H.-N.; Lee, C.-Y.; Chiu, H.-T. Sodium Niobate Nanowire and Its Piezoelectricity. J. Phys. Chem. C 2008, 112, 8827.

(S26) Li, G.; Yang, N.; Wang, W.; Zhang, W. F. Synthesis, Photophysical and Photocatalytic Properties of N-Doped Sodium Niobate Sensitized by Carbon Nitride. J. Phys. Chem. C 2009, 113, 14829.

(S27) Handoko, A. D.; Goh, G. K. L. Hydrothermal Synthesis of Sodium Potassium Niobate Solid Solutions at 200 °C. Green Chem. 2010, 12, 680.

(S28) Wang, G.; Selbach, S. M.; Yu, Y.; Zhang, X.; Grande, T.; Einarsrud, M.-A. Hydrothermal Synthesis and Characterization of $KNbO_3$ Nanorods. CrystEngComm 2009, 11, 1958.

(S29) Mu, W.; Li, X.; Liu, G.; Yu, Q.; Xie, X.; Wei, H.; Jian, Y. Safe Disposal of Radioactive Iodide Ions from Solutions by Ag_2O Grafted Sodium Niobate Nanofibers. Dalton Trans. 2016, 45, 753.

(S30) Lee, Y.; Watanabe, T.; Takata, T.; Kondo, J. N.; Hara, M.; Yoshimura, M.; Domen, K. Preparation and Characterization of Sodium Tantalate Thin Films by Hydrothermal-Electrochemical Synthesis. Chem. Mater. 2005, 17, 2422.

(S31) Kim, S.; Lee, J.-H.; Lee, J.; Kim, S.-W.; Kim, M. H.; Park, S.; Chung, H.; Kim, Y.-I.; Kim, W. Synthesis of Monoclinic Potassium Niobate Nanowires That are Stable at Room Temperature. J. Am. Chem. Soc. 2013, 135, 6.

(S32) Dutto, F.; Raillon, C.; Schenk, K.; Radenovic, A. Nonlinear Optical Response in Single Alkaline Niobate Nanowires. Nano Lett. 2011, 11, 2517.

(S33) Gao, R.; Zhou, S.; Li, W.; Chen, M.; Wu, L. Facile Synthesis of Uniform and Well-Defined Single-Crystal Sodium Tantalate Cubes and Their Assembly into Oriented Two-Dimensional Nanofilm. CrystEngComm 2012, 14, 7031.

(S34) Wang, G.; Yu, Y.; Grande, T.; Einarsrud, M.-A. Synthesis of $KNbO_3$ Nanorods by Hydrothermal Method. J. Nanosci. Nanotechnol. 2009, 9, 1465.

(S35) Shi, H.; Chen, G.; Zhang, C.; Zou, Z. Polymeric g-C_3N_4 Coupled with $NaNbO_3$ Nanowires toward Enhanced Photocatalytic Reduction of CO_2 into Renewable Fuel. ACS Catal. 2014, 4, 3637.

(S36) Kim, S.; Lee, J.-H.; Lee, J.; Kim, S.-W.; Kim, M. H.; Park, S.; Chung, H.; Kim, Y.-I.; Kim, W. Synthesis of Monoclinic Potassium Niobate Nanowires That are Stable at Room Temperature. J. Am. Chem. Soc. 2013, 135, 6.

(S37) Liu, J. W.; Chen, G.; Li, Z. H.; Zhang, Z. G. Hydrothermal Synthesis and Photocatalytic Properties of $ATaO_3$ and $ANbO_3$ (A = Na and K). Int. J. Hydrogen Energy 2007, 32, 2269.

(S38) Zhang, H. J.; Chen, G.; Li, Y. X.; Teng, Y. J. Electronic Structure and Photocatalytic Properties of Copper-Doped $CaTiO_3$. Int. J. Hydrogen Energy 2010, 35, 2713.

(S39) Hu, C. C.; Teng, H. Influence of Structural Features on the Photocatalytic Activity of $NaTaO_3$ Powders from Different Synthesis Methods. Appl. Catal., A 2007, 331, 44.

(S40) Xu, C.-Y.; Zhen, L.; Yang, R.; Wang, Z. L. Synthesis of Single-Crystalline Niobate Nanorods via Ion-Exchange Based on Molten-Salt Reaction. J. Am. Chem. Soc. 2007, 129, 15444.

(S41) Iwase, A.; Kato, H.; Kudo, A. The Effect of Alkaline Earth Metal Ion Dopants on Photocatalytic Water Splitting by $NaTaO_3$ Powder. ChemSusChem 2009, 2, 873.

(S42) Inaba, K.; Suzuki, S.; Noguchi, Y.; Miyayama, M.; Toda, K.; Sato, M. Metastable $Sr_{0.5}TaO_3$ Perovskite Oxides Prepared by Nanosheet Processing. Eur. J. Inorg. Chem. 2008, 2008, 5471.

(S43) Abe, R.; Shinmei, K.; Koumura, N.; Hara, K.; Ohtani, B. Visible-Light-Induced Water Splitting Based on Two-Step Photo-excitation between Dye-Sensitized Layered Niobate and Tungsten Oxide Photocatalysts in the Presence of a Triiodide/Iodide Shuttle Redox Mediator. J. Am. Chem. Soc. 2013, 135, 16872.